

Towards Accurate Acne Detection via Decoupled Sequential Detection Head

Xin Wei¹, Lei Zhang¹, Jianwei Zhang¹, Junyou Wang¹, Wenjie Liu¹, Jiaqi Li² and Xian Jiang²

¹College of Computer Science, Sichuan University, Chengdu 610065, China

²Department of Dermatology, West China Hospital, Sichuan University, Chengdu 610041, China
weixin@stu.scu.edu.cn, leizhang@scu.edu.cn, {zhangjianwei, wangjunyou, liuwj}@stu.scu.edu.cn, lijiaqid@gmail.com, youradrian@outlook.com

Abstract

Accurate acne detection plays a crucial role in acquiring precise diagnosis and conducting proper therapy. However, the ambiguous boundaries and arbitrary dimensions of acne lesions severely limit the performance of existing methods. In this paper, we address these challenges via a novel Decoupled Sequential Detection Head (DSDH), which can be easily adopted by mainstream two-stage detectors. DSDH brings two simple but effective improvements to acne detection. Firstly, the offset and scaling tasks are explicitly introduced, and their incompatibility is settled by our task-decouple mechanism, which improves the capability of predicting the location and size of acne lesions. Second, we propose the task-sequence mechanism, and execute offset and scaling sequentially to gain a more comprehensive insight into the dimensions of acne lesions. In addition, we build a high-quality acne detection dataset named ACNE-DET to verify the effectiveness of DSDH. Experiments on ACNE-DET and the public benchmark ACNE04 show that our method outperforms the state-of-the-art methods by significant margins. Our code and dataset are publicly available at (temporarily anonymous).

1 Introduction

Acne vulgaris, commonly known as acne, is a chronic skin disease characterized by the inflammatory process of hair follicles and sebaceous glands [Zaenglein, 2018]. Epidemiology shows that about 85% of adolescents suffer from acne [Heng and Chew, 2020], which possibly persists through adulthood [Han *et al.*, 2016]. Early intervention is essential for acne patients. Otherwise, both their physical condition and psychological state can be damaged [Dreno *et al.*, 2018; Hazarika and Archana, 2016]. Understanding the status of the facial skin lesions is the basis of evaluating acne severity and conducting further treatment. Nevertheless, since acne patients may need periodic diagnoses, the massive consultation demands are far from being met by dermatologists [Clark *et al.*, 2018]. Therefore, automatic and accurate acne detection algorithms are urgently needed.

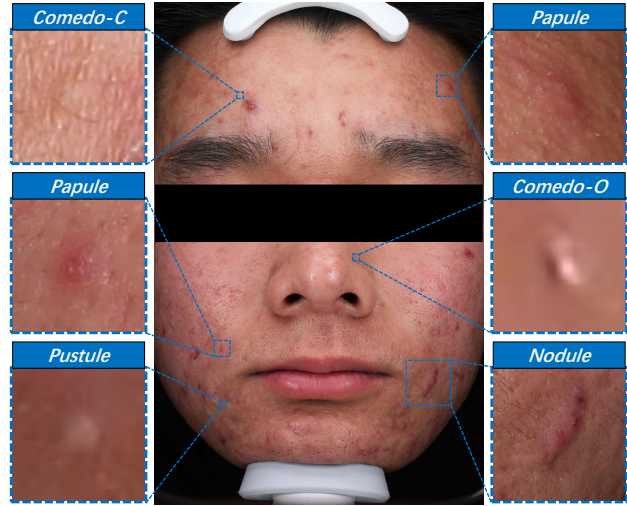


Figure 1: An example of the facial skin images from ACNE-DET. Some acne lesion instances of the example are magnified and shown on the left and right for better clarity.

Traditional acne detection mainly relies on image processing algorithms, which are built on handcrafted features, e.g., color model [Kittigul and Uyyanonvara, 2016], texture-based features [Alamdari *et al.*, 2016] and composited features [Maroni *et al.*, 2017]. But these methods are limited by their weak detection performance and poor generalization capability.

Convolutional neural network (CNN) based methods have achieved significant progress in detecting biomedical objects, such as glomerular [Nguyen *et al.*, 2021], retinopathy [Wang *et al.*, 2017] and universal lesion detection [Yan *et al.*, 2020]. Despite the extensive researches in medical image detection, little attention is paid to acne detection. As a result, only preliminary studies have been made. Wu *et al.* [2019a] construct an acne dataset named ACNE04, which consists of images with detection annotations of a single lesion category, then conduct global acne grading and counting via label distribution learning. Wen *et al.* [2022] and Huynh *et al.* [2022] introduce several generic detection models into acne detection and produce baseline results. Min *et al.* [2021] propose an acne detection network called ACNet consisting of three components, which focus on the issues of imbalanced illumination, lesion variation and dense arrangement, respectively.

However, none of the existing methods effectively address the following challenges: (i) Ambiguous boundaries. There is no clear line of demarcation between the acne lesions and the surrounding normal skin, therefore, even dermatologists sometimes fail to give an accurate answer on the location and size of an acne lesion. (ii) Arbitrary dimensions. A large acne lesion may occupy an entire patch of skin, while a small acne lesion can be hard to see with naked eyes, which implies the dimensions of the acne lesions vary widely. (iii) Lack of datasets. Publicly available acne datasets, especially high-quality ones, are extremely scarce due to the complexity of whole-face annotation, thus severely impeding the development of acne detection. Some acne lesion instances are presented in Figure 1 for illustration.

Based on the above discussions, the limited performance of existing acne detection methods motivates us to optimize the architectures of generic detection models and construct a new dataset for acne detection. The main contributions of this paper are summarized as follows:

- We explicitly introduce the offset task and the scaling task, and decouple them by two standalone branches to settle their incompatibility. The task-decouple mechanism effectively improves the capability of the detection head to predict the location and size of the acne lesions.
- We split the bounding box refinement task into two steps, and execute the offset task and the scaling task sequentially to facilitate scaling. The task-sequence mechanism enables the detection head to gain a more comprehensive insight into the dimensions of the acne lesions.
- We build a high-quality acne detection dataset named *ACNE-DET* to verify the effectiveness of our methods. *ACNE-DET* surpasses the previous acne dataset for its high-resolution facial skin images, superior annotation accuracy and fine-grained skin lesion categories.

By combining the task-decouple and task-sequence mechanisms, we propose a novel Decoupled Sequential Detection Head (DSDH), which can be easily adopted by mainstream two-stage detectors. Comprehensive experiments on both *ACNE-DET* and *ACNE04* show that our method outperforms the state-of-the-art methods by significant margins.

2 Related Works

2.1 Object Detection

Recent object detection algorithms are mainly based on CNN, and are divided into two categories according to their network architectures.

One-stage Methods. One-stage methods formulate object detection as an end-to-end task. Thus, the classification and bounding box results are obtained in a single network. YOLO [Redmon *et al.*, 2016] introduces a unified network to object detection for the first time. SSD [Liu *et al.*, 2016] optimizes the object matching quality by generating anchor boxes of different sizes and aspect ratios. RetinaNet [Lin *et al.*, 2017] constructs focal loss, which alleviates the foreground-background class imbalance. FCOS [Tian *et al.*, 2019] directly predicts at every position of the feature map and builds the anchor free detection framework.

Two-stage Methods. Two-stage methods implement object detection in two steps: (i) region proposal with raw bounding boxes and (ii) region-based classification and bounding box refinement. For the first time, RCNN [Girshick *et al.*, 2014] applies CNN to extract features from regions proposed by the selective search. SPPNet [He *et al.*, 2015] forwards the whole image through the network and introduces spatial pyramid pooling. Fast RCNN [Girshick, 2015] adopts RoI-pooling, which is a differentiable layer, and thus speeds up the network significantly. Faster RCNN [Ren *et al.*, 2015] further improves the detection efficiency by replacing the selective search with the region proposal network. R-FCN [Dai *et al.*, 2016] designs position sensitive RoI-pooling to deal with the translation-variance. Mask RCNN [He *et al.*, 2017] employs RoI-align instead of RoI-pooling, eliminating the misalignment caused by the quantitative operations.

Although one-stage methods have higher inference speeds, they are generally less likely to produce state-of-the-art results than two-stage methods. Since the acne detection task is insensitive to inference speed, our research mainly focuses on two-stage methods.

2.2 Detection Head

As the prediction module of the object detection framework, the detection head has drawn much attention. By constructing a sequence of detection heads trained with increasing IoU thresholds, Cascade RCNN [Cai and Vasconcelos, 2018] achieves better object matching quality stage by stage. IoU-Net [Jiang *et al.*, 2018] applies an extra branch to predict IoUs between detected bounding boxes and their corresponding ground truths. Similar to IoU-Net, Mask Scoring RCNN [Huang *et al.*, 2019] presents mask IoU scores for each segmentation mask. Double-Head [Wu *et al.*, 2020] employs two standalone branches to generate the refined bounding box and classification results. D2Det [Cao *et al.*, 2020] adopts a dense detection head that predicts multiple box offsets for a proposal. EFLDet [Liao *et al.*, 2021] proposes a trident head to integrate diverse information from the feature maps.

However, the existing methods all neglect two significant defects of the proposed detection heads: (i) as two separate subtasks of bounding box refinement, offset and scaling are coupled in the same branch and (ii) the potential sequential relevance of offset and scaling is not taken into account. To settle the above defects of the mainstream detection heads and promote acne detection, we implement exhaustive studies and conduct experiments on multiple datasets.

3 Methodology

To tackle the issues of ambiguous boundaries and arbitrary dimensions of the acne lesions, we conduct a thorough analysis on the detection heads of mainstream two-stage detectors and further develop an optimized detection head paradigm. In this section, we first elaborate the incompatibility between the offset and scaling tasks, and introduce the task-decouple mechanism. Next, we analyze the potential sequential relevance of offset and scaling, and present the task-sequence mechanism. Finally, Decoupled Sequential Detection Head (DSDH) is proposed by combining the mechanisms above, and the overall architecture is illustrated in Figure 2(e).

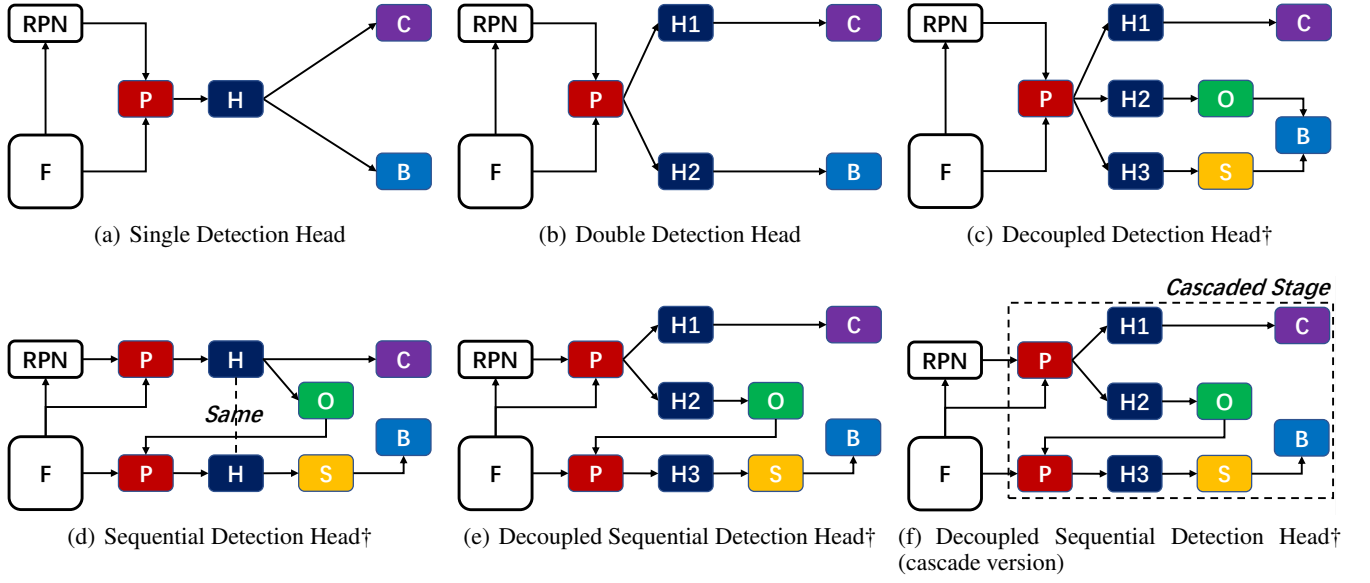


Figure 2: Comparisons of different detection head architectures. “F” for feature maps extracted by backbone. “RPN” for a region proposal network. “P” for a pooling operator, e.g., ROI-pooling or RoI-align. “H” for a network branch of detection head. “C” for classification results. “B” for bounding box results. “O” for offset results. “S” for scaling results. † indicates our methods.

3.1 Task-Decouple Mechanism

In the two-stage detection framework, the first stage is a region proposal network (RPN), which generates raw proposal bounding boxes $B_p = (x_p, y_p, w_p, h_p)$. In order to fit the corresponding ground truth bounding boxes $B_g = (x_g, y_g, w_g, h_g)$ and the classifications C_g , a region-based network known as the detection head is employed in the second stage. The difference $\Delta = (\delta_x, \delta_y, \delta_w, \delta_h)$ between B_p and B_g is defined as

$$\begin{aligned} \delta_x &= \lambda_x (x_g - x_p) / w_p, & \delta_y &= \lambda_y (y_g - y_p) / h_p, \\ \delta_w &= \lambda_w \log(w_g / w_p), & \delta_h &= \lambda_h \log(h_g / h_p), \end{aligned} \quad (1)$$

where x_p, y_p, w_p and h_p represent the abscissa, ordinate, width and height of B_p respectively (likewise for B_g), and $\lambda_x, \lambda_y, \lambda_w$ and λ_h represent the corresponding standard deviations, which are typically used as scalars 10, 10, 5 and 5 in previous works [Huang *et al.*, 2017].

Adopting a detection head with only a single network branch is a simple way to fit the difference Δ . In this framework, a pooling operator P is employed to extract proposal features F_p from backbone feature maps F based on proposal bounding boxes B_p . Then, a single branch H is deployed to generate refined bounding boxes B and classifications C simultaneously, during which a post-processor T transforms the original bounding boxes into the target bounding boxes. This framework is utilized by mainstream methods such as Faster RCNN [Ren *et al.*, 2015] and Mask RCNN [He *et al.*, 2017] and summarized as Single Detection Head, whose pipeline is depicted in Figure 2(a) and formulated as

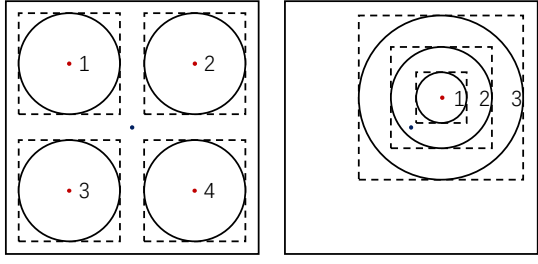
$$F_p = P(F, B_p), C = H(F_p), B = T(B_p, H(F_p)). \quad (2)$$

Driven by the weak performance of Single Detection Head, some researchers focus on the sibling tasks, i.e., bounding

box refinement and classification. They find that the essential barrier lies in the incompatibility between these two tasks. As two separate tasks, bounding box refinement and classification aim to fit two distinct inherent attributes of objects, but are tangled in the same branch. Wu *et al.* [2020] and Song *et al.* [2020] introduce two standalone branches H_1 and H_2 to disentangle the sibling tasks, which effectively alleviates the incompatibility between them. This framework is summarized as Double Detection Head, whose pipeline is depicted in Figure 2(b) and formulated as

$$F_p = P(F, B_p), C = H_1(F_p), B = T(B_p, H_2(F_p)). \quad (3)$$

Despite the merits revealed in Double Detection Head, the incompatibility between the subtasks of bounding box refinement is still neglected. We propose the **task-decouple mechanism** to settle this defect. As four separate components of the difference Δ , $\delta_x, \delta_y, \delta_w$ and δ_h can be naturally categorized into the offset component $O = (\delta_x, \delta_y)$ and the scaling component $S = (\delta_w, \delta_h)$, where $\Delta = (O, S)$. Through this decomposition, we divide the bounding box refinement task into the offset and the scaling subtasks. Inspired by the double-head approaches, we evaluate their incompatibility. Figure 3 illustrates that whatever the situation is, the difference between the proposals and the ground truths can always be fitted by two uncorrelated subtasks, i.e., offset and scaling, representing the variations of location and size respectively. Therefore, they should not be coupled in the same branch. To further decouple offset and scaling, we deploy two standalone branches H_2 and H_3 parallelly, with the classification branch H_1 remaining independent. The proposed framework is denoted as Decoupled Detection Head, whose pipeline is depicted in Figure 2(c) and formulated as (the classification branch H_1 is omitted in the formula as it is not the primary



(a) Situations with the same scaling and different offset (b) Situations with the same offset and different scaling

Figure 3: Situations with various offset and scaling. The outer solid rectangles represent the proposal bounding boxes. The solid circles represent the simplified acne samples. The dotted rectangles represent the ground truth bounding boxes corresponding to the acne samples. The blue and red dots represent the center points of the proposals and ground truths, respectively. The numbers indicate the situations the acne samples may exhibit in the proposals.

research focus, the same hereafter)

$$\begin{aligned} F_p &= P(F, B_p), & O &= H_2(F_p), \\ S &= H_3(F_p), & B &= T(B_p, (O, S)). \end{aligned} \quad (4)$$

The task-decouple mechanism effectively alleviates the incompatibility between the offset task and the scaling task, and thus improves the capability of the detection head to predict the location and size of the acne lesions.

3.2 Task-Sequence Mechanism

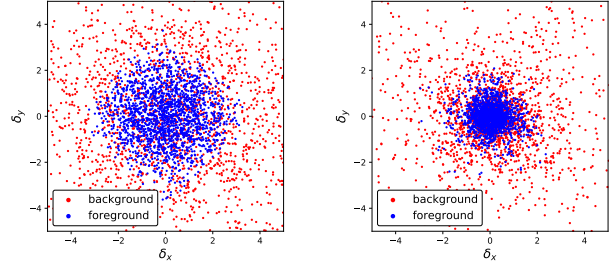
Another significant defect of the mainstream detection heads is that the subtasks of bounding box refinement are executed parallelly, without their potential sequential relevance taken into account. We propose the **task-sequence mechanism** to tackle this issue. Based on the conditional probability formula, we can conclude that

$$p(O, S) = p(O)p(S | O). \quad (5)$$

Following this formula, the bounding box refinement task is split into two steps: (i) generate the offset component O on the basis of proposals and (ii) generate the scaling component S under the condition of O . Through this formulation, we execute the offset task and the scaling task sequentially.

In fact, with the help of the offset task, we can facilitate the scaling task. As shown in Figure 4, the absolute values of the components δ_x and δ_y decrease sharply after we execute the offset task, which means that the proposals get closer to the ground truths. Therefore, the scaling task is facilitated from two aspects. On the one hand, the ground truths area which appears in the proposals is increased, resulting in richer features. Intuitively, the size of an object with its entire portion in the field of view is more predictable than one with only a small portion. On the other hand, with the distributions of the ground truths converging towards the center of proposals, the requirements for the generalization capability of detection heads are also reduced.

In our sequential framework, we first execute the offset task to generate the offset component O , based on which the post-processor T refines the proposal bounding boxes B_p to B_o



(a) Before executing offset (b) After executing offset

Figure 4: Distributions of the components δ_x and δ_y before and after we execute the offset task. The background and foreground samples are divided by IoU=0.5 in the training phase.

in its location. Next, F_o are extracted as the corresponding features of B_o . At last, we execute the scaling task to generate the scaling component S , based on which T refines B_o to the refined bounding boxes B in its size. Note that all tasks share the same branch H in this formulation. The proposed framework is denoted as Sequential Detection Head, whose pipeline is depicted in Figure 2(d) and formulated as

$$\begin{aligned} F_p &= P(F, B_p), & O &= H(F_p), & B_o &= T(B_p, O), \\ F_o &= P(F, B_o), & S &= H(F_o), & B &= T(B_o, S). \end{aligned} \quad (6)$$

The task-sequence mechanism facilitates the scaling task, enabling the detection head to gain a more comprehensive insight into the dimensions of the acne lesions.

3.3 Decoupled Sequential Detection Head

Utilizing the task-decouple and task-sequence mechanisms simultaneously, we propose a novel Decoupled Sequential Detection Head (DSDH). In this framework, the offset task and the scaling task are not only decoupled by two standalone branches, but also executed sequentially. Meanwhile, the classification branch remains independent. The pipeline of DSDH is depicted in Figure 2(e) and formulated as

$$\begin{aligned} F_p &= P(F, B_p), & O &= H_2(F_p), & B_o &= T(B_p, O), \\ F_o &= P(F, B_o), & S &= H_3(F_o), & B &= T(B_o, S). \end{aligned} \quad (7)$$

Since all the modules described above are differentiable, DSDH is trained in an end-to-end manner and optimized by the following multi-task loss

$$\mathcal{L} = \mathcal{L}_{cls} + \alpha \mathcal{L}_{off} + \beta \mathcal{L}_{sca}, \quad (8)$$

where \mathcal{L}_{off} and \mathcal{L}_{sca} represent the losses for the offset task and the scaling task respectively, and \mathcal{L}_{cls} for the loss of the classification task. The coefficients α and β are employed to balance the offset task and the scaling task. We set $\alpha = 1$ and $\beta = 1$ by default.

In addition, for the sake of inspecting whether DSDH can be further enhanced by the cascade architecture that is commonly used in general-purpose detection frameworks, we refer to the paradigm presented in [Cai and Vasconcelos, 2018] and construct the cascade version of DSDH, whose pipeline is depicted in Figure 2(f).

DSDH aims to tackle the issues of ambiguous boundaries and arbitrary dimensions of the acne lesions through two simple but effective improvements, and it can be easily adopted by mainstream two-stage detectors.

	Detector	AP	AP_S	AP_M	AP_L
One-stage methods	FCOS [Tian <i>et al.</i> , 2019]	40.2	39.1	44.5	22.9
	RetinaNet [Lin <i>et al.</i> , 2017]	41.1	40.1	46.1	24.0
Two-stage methods	Cascade RCNN [Cai and Vasconcelos, 2018]	42.4	41.9	41.8	29.9
	Faster RCNN w/o FPN [Ren <i>et al.</i> , 2015]	34.4	29.8	38.6	29.4
	Faster RCNN [Ren <i>et al.</i> , 2015]	41.9	40.4	43.7	29.1
	Mask RCNN [He <i>et al.</i> , 2017]	43.3	42.7	43.1	30.9
	Double-Head [Wu <i>et al.</i> , 2020]	43.8	44.1	44.3	29.2
	Double-FC [Wu <i>et al.</i> , 2020]	44.0	43.7	45.3	30.1
Our methods	Cascade RCNN + DSDH	43.8	42.6	43.9	31.5
	Faster RCNN + DSDH	44.4	43.7	45.8	29.0
	Mask RCNN + DSDH	45.6	44.3	46.9	34.1

Table 1: Comparisons with various state-of-the-art methods on *ACNE-DET*. All models utilize ResNet-50 backbone.

Detector	Backbone	AP
R-FCN [Dai <i>et al.</i> , 2016]	ResNet-101	14.0
Rashataprucksa <i>et al.</i> [2020]	ResNet-101	14.7
ACNet [Min <i>et al.</i> , 2021]	ResNet-101*	20.5
Mask RCNN + DSDH†	ResNet-101	23.0

Table 2: Comparisons with state-of-the-art methods on *ACNE04*. * indicates an enhanced backbone. † indicates our method.

4 Experiments

In this section, we first detail the datasets. Then, we describe the implementation details and evaluation metrics. Finally, several experiments are presented.

4.1 Datasets

The ACNE-DET Dataset. Due to the absence of high-quality acne detection datasets, our work begins with the construction of a new dataset named *ACNE-DET*, which has the following merits: Firstly, through VISIA, a professional facial skin image acquisition equipment, we collect a batch of high-quality skin images characterized by standardization, high-resolution and no redundant information. Second, these skin images have undergone multiple rounds of annotation and modification by six dermatologists on our specialized acne annotation system, so they have superior annotation accuracy. Finally, to exhaustively analyze the skin lesions, we divide them into ten fine-grained categories, including *Close Comedo (Comedo-C)*, *Open Comedo (Comedo-O)*, *Papule, Pustule, Nodule, Atrophic Scar (Scar-A)*, *Hypertrophic Scar (Scar-H)*, *Melasma, Nevus* and *Other*. They comprise both common acne and non-acne skin lesion categories. Note that the skin lesions without a certain category are labeled as *Other*. *ACNE-DET* contains 276 facial skin images with 31,777 labeled lesion instances. An example of the facial skin images from *ACNE-DET* is shown in Figure 1. We randomly divide *ACNE-DET* into a testing set and a training set which contains 241 labeled images with 28,260 skin lesions of various forms and sizes. Since the same patient may be examined multiple times, resulting in correlated data, we guarantee the data of the same patient to appear in only one dataset.

Decouple	Sequence	AP	AP_S	AP_M	AP_L
		43.3	42.7	43.1	30.9
	✓	44.7	43.2	44.2	32.9
✓		44.8	44.5	44.5	32.9
✓	✓	45.6	44.3	46.9	34.1

Table 3: Ablation study of the model design on *ACNE-DET*. The base model is “Mask RCNN + DSDH” with ResNet-50 backbone.

The ACNE04 Dataset. In order to verify the effectiveness of DSDH, we employ *ACNE04* [Wu *et al.*, 2019a] as a public benchmark of acne detection. *ACNE04* contains 1,457 skin images collected by digital cameras with 18,983 bounding box annotations of a single lesion category. Following [Min *et al.*, 2021], we randomly split the dataset into 80% training set and 20% testing set, and further crop the images into 640×640 sub-images.

4.2 Implementation Details

Our work is conducted based on Detectron2 [Wu *et al.*, 2019b] and trained on an NVIDIA 3090 GPU. The pre-trained parameters from COCO [Lin *et al.*, 2014] are employed to initialize all models. The horizontal flip is used in the data augmentation, and a learning rate of $2e - 3$ with a momentum of 0.9 is adopted in the 13 epochs training. The ratio of background and foreground samples fed into the detection head is 3. NMS threshold is set to IoU=0.5 in the testing phase, and bounding boxes with classification scores greater than 0.01 are output as the detection results.

4.3 Evaluation Metrics

As the primary metric of object detection, mean Average Precision (AP) is commonly used to measure the performance across all categories [Wang *et al.*, 2022; Xiong *et al.*, 2022]. We utilize PASCAL-style AP as the main evaluation metric of acne detection. In addition, we evaluate the performance on acne lesions in various sizes through AP_S , AP_M and AP_L , which are AP for small objects (area less than 32^2), medium objects (area between 32^2 and 96^2) and large objects (area greater than 96^2), respectively. The maximum number of the bounding boxes participating in the evaluation is 100.

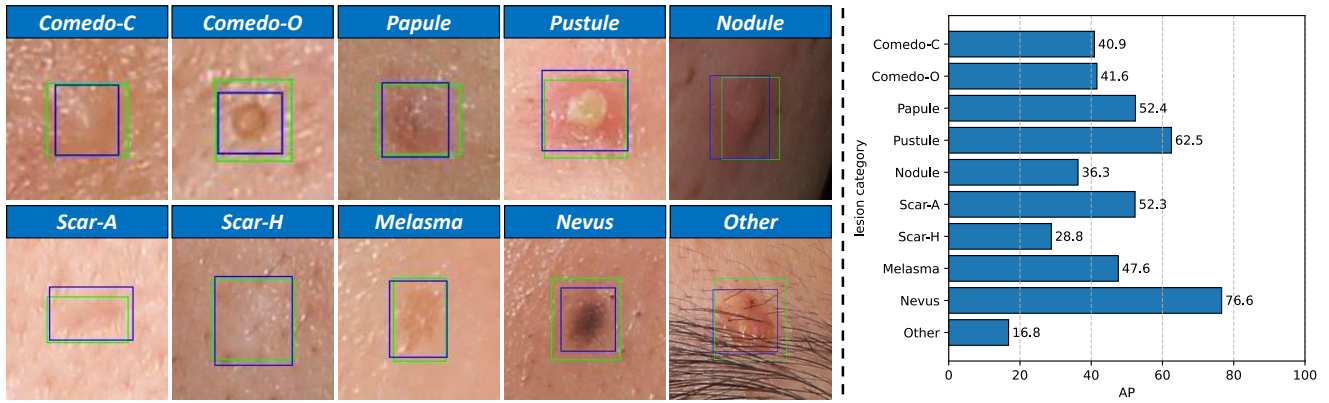


Figure 5: Visualization results by lesion category on *ACNE-DET*. Left: visualization of the qualitative results. Examples of the skin lesions are cropped from the original images by category and magnified for better clarity. The bounding boxes of the ground truth and our method are marked by the green and blue rectangles, respectively. Right: visualization of the quantitative results.

Conv	FC	AP	AP_S	AP_M	AP_L
0	1	45.0	44.5	48.3	33.1
	2	45.6	44.3	46.9	34.1
1	1	44.7	43.7	46.4	33.1
	2	44.1	42.9	45.7	32.6
2	1	44.6	42.8	47.4	33.9
	2	44.0	42.5	45.4	32.7

Table 4: Ablation study of the branch network on *ACNE-DET*. The base model is “Mask RCNN + DSDH” with ResNet-50 backbone.

4.4 Main Results

Comparisons with State-of-the-art Methods. As the representative works of two-stage detectors, Faster RCNN [Ren *et al.*, 2015] and Cascade RCNN [Cai and Vasconcelos, 2018] are employed in the experiment on *ACNE-DET*. Mask RCNN [He *et al.*, 2017] is also included as an enhanced version of Faster RCNN. Then, we replace the original detection heads of the above detectors with DSDH to verify its effectiveness. Another state-of-the-art detector, namely Double-Head, and its variation Double-FC [Wu *et al.*, 2020] are also utilized. Besides, FCOS [Tian *et al.*, 2019] and RetinaNet [Lin *et al.*, 2017] are chosen as the representative works of the one-stage detectors. Note that we try our best to implement the compared methods with the same hyper-parameters and settings. As shown in Table 1, our method achieves state-of-the-art results compared with both one-stage and two-stage methods, utilizing the same ResNet-50 backbone. Specifically, Mask RCNN based DSDH outperforms all other methods, and improves AP by 2.3%, AP_S , AP_M and AP_L by 1.6%, 3.8% and 3.2% respectively compared with the original Mask RCNN. It should be noted that this is actually a significant progress. In fact, even dermatologists sometimes fail to label consistent ground truths due to the ambiguous boundaries of the acne lesions, thus severely impeding the performance gains. Furthermore, Faster RCNN based DSDH and Cascade RCNN based DSDH surpass the original versions by 2.5% and 1.4% respectively, demonstrating the generalization capability of our

Backbone	AP	AP_S	AP_M	AP_L
ResNet-50	45.6	44.3	46.9	34.1
ResNet-101	45.2	43.9	46.2	32.5
ResNeXt-101	42.8	44.2	45.0	26.4

Table 5: Ablation study of the backbone scale on *ACNE-DET*. The base model is “Mask RCNN + DSDH.”

method. We believe DSDH effectively alleviates the incompatibility between the offset and scaling tasks, and further facilitates the scaling task in acne detection. Notably, two-stage detectors achieve better results than one-stage detectors, especially on AP_L . This may attribute to the universality of the two-stage detectors. It is noticed that, with or without DSDH, the cascade detectors perform worse than the vanilla ones. We argue that the increasing IoU thresholds are unsuitable for acne detection due to the ambiguous boundaries.

Visualization Results by Lesion Category. The results of our Mask RCNN based DSDH are visualized in Figure 5 to illustrate the detection performance for each lesion category. We can see that our method works well for most categories, and even fits the skin lesion areas better than the ground truths labeled by the dermatologists in some cases, which exhibits the high performance of the proposed DSDH on acne detection. Note that AP of *Other* is relatively low since it consists of various lesion categories.

Comparison Results on ACNE04. To further demonstrate the effectiveness of our method, we compare Mask RCNN based DSDH with the detection methods that have published results on *ACNE04*. As shown in Table 2, our method outperforms all the prior state-of-the-art methods by large margins, without bells and whistles.

4.5 Ablation Studies

We perform groups of ablation studies on *ACNE-DET* to analyze the optimal design of our method. Mask RCNN based DSDH is chosen as the base model in the following experiments for its best performance.

Decouple Manner	AP	AP_s	AP_m	AP_l
No decouple [He <i>et al.</i> , 2017]	43.3	42.7	43.1	30.9
Double-FC [Wu <i>et al.</i> , 2020]	44.0	43.7	45.3	30.1
Offset plus scaling [†]	44.8	44.5	44.5	32.9
Horizontal plus vertical [†]	44.3	44.2	46.0	32.5
Fully decoupled [†]	44.3	44.0	45.1	31.0

Table 6: Evaluations of various decouple manner on *ACNE-DET*. “No decouple” represents Mask RCNN. [†] indicates our variations.

Model Design. We omit different components in DSDH, including the task-decouple mechanism and task-sequence mechanism, to investigate their effectiveness. Results are shown in Table 3. The task-decouple mechanism gains AP by 1.5%, while the task-sequence mechanism leads to a gain of 1.3%. These two mechanisms both prove their ability to enhance acne detection. Furthermore, they can achieve mutual benefit when combined.

Branch Network. We design the structure of the branch networks by exploring the layer numbers, on the premise that the channel numbers of the convolutional layers and the fully connected layers are fixed at 256 and 1024, respectively. From Table 4, we can learn that with the number of convolutional layers increasing, the performance of the model declines. We adopt “Conv-0 FC-2” in all branches for its superior performance. Note that this is the default setting of the two-stage methods shown in Table 1, except Double-Head.

Backbone Scale. Table 5 shows the comparisons of different backbone scales. ResNet-50, ResNet-101 and ResNeXt-101 [Xie *et al.*, 2017] 32x8d are utilized as the competitors, among which ResNet-50 takes the lead on all metrics.

4.6 Structure Variations

To gain a more comprehensive understanding of our approach, we explore the variations of the task-decouple and the task-sequence manners. Explorations are based on Mask RCNN with ResNet-50 backbone on *ACNE-DET*.

Variations of Task-Decouple. We discuss the variations of task-decouple manner of the bounding box refinement task. Three variations are explained as follows:

- Offset plus scaling: the bounding box refinement task is divided into the offset and the scaling subtasks, which are decoupled by two standalone branches (our choice).
- Horizontal plus vertical: the bounding box refinement task is divided into the horizontal and the vertical subtasks, which are decoupled by two standalone branches.
- Fully decoupled: the subtasks of bounding box refinement are fully decoupled by four standalone branches.

where the horizontal task and the vertical task consist of the subtasks relevant to x-axis and y-axis, respectively (i.e., decompose Δ into $\mathcal{H} = (\delta_x, \delta_w)$ and $\mathcal{V} = (\delta_y, \delta_h)$). Note that the task-sequence mechanism is not implemented, and the classification branch is independent in the above variations.

Results are shown in Table 6. “No decouple” (i.e., Mask RCNN) and Double-FC are listed as the baseline methods.

Sequence Manner	AP	AP_s	AP_m	AP_l
Parallel [He <i>et al.</i> , 2017]	43.3	42.7	43.1	30.9
Offset then scaling [†]	44.7	43.2	44.2	32.9
Scaling then offset [†]	44.2	43.2	45.3	31.6
Horizontal then vertical [†]	44.0	42.9	46.1	31.7
Vertical then horizontal [†]	44.2	42.9	45.9	32.3

Table 7: Evaluations of various sequence manner on *ACNE-DET*. “Parallel” represents Mask RCNN. [†] indicates our variations.

We can learn all variations achieve performance gains over the baseline methods, with “Offset plus scaling” taking the lead. Results demonstrate that “Offset plus scaling,” adopted in our task-decouple mechanism, is the optimal option and alleviates the incompatibility between offset and scaling.

Variations of Task-Sequence. The variations of the task-sequence manner are analyzed after we split the bounding box refinement task into two steps. Four variations are explained as follows:

- Offset then scaling: execute the offset task first, then the scaling task (our choice).
- Scaling then offset: execute the scaling task first, then the offset task.
- Horizontal then vertical: execute the horizontal task first, then the vertical task.
- Vertical then horizontal: execute the vertical task first, then the horizontal task.

Note that the task-decouple mechanism is not implemented in the above variations, which means that all tasks share the same branch.

As shown in Table 7, all variations obtain better results compared with the baseline method “Parallel” (i.e., Mask RCNN), among which “Offset then scaling” performs best. Results verify our opinion that “Offset then scaling” effectively facilitates the scaling task, and is the best choice for our task-sequence mechanism.

5 Conclusion and Future Research

In this paper, we propose a novel Decoupled Sequential Detection Head (DSDH) for acne detection. DSDH tackles the issues of ambiguous boundaries and arbitrary dimensions of the acne lesions via two simple but effective improvements. Our task-decouple mechanism settles the incompatibility between the offset and scaling tasks to improve the capability of predicting the location and size of acne lesions. Utilizing the task-sequence mechanism, we execute offset and scaling sequentially to gain a more comprehensive insight into the dimensions of acne lesions. In addition, we construct a high-quality acne detection dataset named ACNE-DET to verify the effectiveness of DSDH. Experiments show our method significantly outperforms the state-of-the-art methods.

DSDH optimizes the architectures of conventional detection heads, and can be easily adopted by mainstream two-stage detectors. In future research, it is worth exploring the capability of DSDH as a general-purpose detection head.

References

- [Alamdari *et al.*, 2016] Nasim Alamdari, Kouhyar Tavakolian, Minhal Alhashim, and Reza Fazel-Rezai. Detection and classification of acne lesions in acne patients: A mobile application. In *2016 IEEE international conference on electro information technology (EIT)*, pages 0739–0743. IEEE, 2016.
- [Cai and Vasconcelos, 2018] Zhaowei Cai and Nuno Vasconcelos. Cascade r-cnn: Delving into high quality object detection. In *Proceedings of the IEEE conference on computer vision and pattern recognition (CVPR)*, pages 6154–6162, 2018.
- [Cao *et al.*, 2020] Jiale Cao, Hisham Cholakkal, Rao Muhammad Anwer, Fahad Shahbaz Khan, Yanwei Pang, and Ling Shao. D2det: Towards high quality object detection and instance segmentation. In *Proceedings of the IEEE conference on computer vision and pattern recognition (CVPR)*, pages 11485–11494, 2020.
- [Clark *et al.*, 2018] Ashley K Clark, Suzana Saric, and Raja K Sivamani. Acne scars: how do we grade them? *American Journal of Clinical Dermatology*, 19(2):139–144, 2018.
- [Dai *et al.*, 2016] Jifeng Dai, Yi Li, Kaiming He, and Jian Sun. R-fcn: Object detection via region-based fully convolutional networks. *Advances in neural information processing systems*, 29, 2016.
- [Dreno *et al.*, 2018] Brigitte Dreno, Edileia Bagatin, Ulrike Blume-Peytavi, Marco Rocha, and Harald Gollnick. Female type of adult acne: Physiological and psychological considerations and management. *JDDG: Journal der Deutschen Dermatologischen Gesellschaft*, 16(10):1185–1194, 2018.
- [Girshick *et al.*, 2014] Ross Girshick, Jeff Donahue, Trevor Darrell, and Jitendra Malik. Rich feature hierarchies for accurate object detection and semantic segmentation. In *Proceedings of the IEEE conference on computer vision and pattern recognition (CVPR)*, pages 580–587, 2014.
- [Girshick, 2015] Ross Girshick. Fast r-cnn. In *Proceedings of the IEEE international conference on computer vision (ICCV)*, pages 1440–1448, 2015.
- [Han *et al.*, 2016] XD Han, HH Oon, and CL Goh. Epidemiology of post-adolescence acne and adolescence acne in singapore: a 10-year retrospective and comparative study. *Journal of the European Academy of Dermatology and Venereology*, 30(10):1790–1793, 2016.
- [Hazarika and Archana, 2016] N Hazarika and M Archana. The psychosocial impact of acne vulgaris. *Indian journal of dermatology*, 61(5):515, 2016.
- [He *et al.*, 2015] Kaiming He, Xiangyu Zhang, Shaoqing Ren, and Jian Sun. Spatial pyramid pooling in deep convolutional networks for visual recognition. *IEEE transactions on pattern analysis and machine intelligence (TPAMI)*, 37(9):1904–1916, 2015.
- [He *et al.*, 2017] Kaiming He, Georgia Gkioxari, Piotr Dollár, and Ross Girshick. Mask r-cnn. In *Proceedings of the IEEE international conference on computer vision (ICCV)*, pages 2961–2969, 2017.
- [Heng and Chew, 2020] AHS Heng and Fook Tim Chew. Systematic review of the epidemiology of acne vulgaris. *Scientific reports*, 10(1):1–29, 2020.
- [Huang *et al.*, 2017] Jonathan Huang, Vivek Rathod, Chen Sun, Menglong Zhu, Anoop Korattikara, Alireza Fathi, Ian Fischer, Zbigniew Wojna, Yang Song, Sergio Guadarrama, et al. Speed/accuracy trade-offs for modern convolutional object detectors. In *Proceedings of the IEEE conference on computer vision and pattern recognition (CVPR)*, pages 7310–7311, 2017.
- [Huang *et al.*, 2019] Zhaojin Huang, Lichao Huang, Yongchao Gong, Chang Huang, and Xinggang Wang. Mask scoring r-cnn. In *Proceedings of the IEEE conference on computer vision and pattern recognition (CVPR)*, pages 6409–6418, 2019.
- [Huynh *et al.*, 2022] Quan Thanh Huynh, Phuc Hoang Nguyen, Hieu Xuan Le, Lua Thi Ngo, Nhu-Thuy Trinh, Mai Thi-Thanh Tran, Hoan Tam Nguyen, Nga Thi Vu, Anh Tam Nguyen, Kazuma Suda, et al. Automatic acne object detection and acne severity grading using smartphone images and artificial intelligence. *Diagnostics*, 12(8):1879, 2022.
- [Jiang *et al.*, 2018] Borui Jiang, Ruixuan Luo, Jiayuan Mao, Tete Xiao, and Yuning Jiang. Acquisition of localization confidence for accurate object detection. In *Proceedings of the european conference on computer vision (ECCV)*, pages 784–799, 2018.
- [Kittigul and Uyyanonvara, 2016] Natchapol Kittigul and Bunyarit Uyyanonvara. Automatic acne detection system for medical treatment progress report. In *2016 7th International Conference of Information and Communication Technology for Embedded Systems (IC-ICTES)*, pages 41–44. IEEE, 2016.
- [Liao *et al.*, 2021] Yongwei Liao, Guipeng Zhang, Zhenguo Yang, and Wenyan Liu. Efldet: enhanced feature learning for object detection. *Neural Computing and Applications*, pages 1–13, 2021.
- [Lin *et al.*, 2014] Tsung-Yi Lin, Michael Maire, Serge Belongie, James Hays, Pietro Perona, Deva Ramanan, Piotr Dollár, and C Lawrence Zitnick. Microsoft coco: Common objects in context. In *ECCV*, pages 740–755. Springer, 2014.
- [Lin *et al.*, 2017] Tsung-Yi Lin, Priya Goyal, Ross Girshick, Kaiming He, and Piotr Dollár. Focal loss for dense object detection. In *Proceedings of the IEEE international conference on computer vision (ICCV)*, pages 2980–2988, 2017.
- [Liu *et al.*, 2016] Wei Liu, Dragomir Anguelov, Dumitru Erhan, Christian Szegedy, Scott Reed, Cheng-Yang Fu, and Alexander C Berg. Ssd: Single shot multibox detector. In *european conference on computer vision (ECCV)*, pages 21–37. Springer, 2016.

- [Maroni *et al.*, 2017] Gabriele Maroni, Michele Ermidoro, Fabio Previdi, and Glauco Bigini. Automated detection, extraction and counting of acne lesions for automatic evaluation and tracking of acne severity. In *2017 IEEE symposium series on computational intelligence (SSCI)*, pages 1–6. IEEE, 2017.
- [Min *et al.*, 2021] Kyungseo Min, Gun-Hee Lee, and Seong-Whan Lee. Acnet: Mask-aware attention with dynamic context enhancement for robust acne detection. In *2021 IEEE International Conference on Systems, Man, and Cybernetics (SMC)*, pages 2724–2729. IEEE, 2021.
- [Nguyen *et al.*, 2021] Ethan H Nguyen, Haichun Yang, Ruining Deng, Yuzhe Lu, Zheyu Zhu, Joseph T Roland, Le Lu, Bennett A Landman, Agnes B Fogo, and Yuankai Huo. Circle representation for medical object detection. *IEEE Transactions on Medical Imaging (TMI)*, 41(3):746–754, 2021.
- [Rashataprucksa *et al.*, 2020] Kuladech Rashataprucksa, Chavalit Chuangchaichatchavarn, Sipat Triukose, Sirin Nitinawarat, Marisa Pongprutthipan, and Krerk Piromsopa. Acne detection with deep neural networks. In *2020 2nd International Conference on Image Processing and Machine Vision*, pages 53–56, 2020.
- [Redmon *et al.*, 2016] Joseph Redmon, Santosh Divvala, Ross Girshick, and Ali Farhadi. You only look once: Unified, real-time object detection. In *Proceedings of the IEEE conference on computer vision and pattern recognition (CVPR)*, pages 779–788, 2016.
- [Ren *et al.*, 2015] Shaoqing Ren, Kaiming He, Ross Girshick, and Jian Sun. Faster r-cnn: Towards real-time object detection with region proposal networks. *Advances in neural information processing systems*, 28, 2015.
- [Song *et al.*, 2020] Guanglu Song, Yu Liu, and Xiaogang Wang. Revisiting the sibling head in object detector. In *Proceedings of the IEEE conference on computer vision and pattern recognition (CVPR)*, pages 11563–11572, 2020.
- [Tian *et al.*, 2019] Zhi Tian, Chunhua Shen, Hao Chen, and Tong He. Fcos: Fully convolutional one-stage object detection. In *Proceedings of the IEEE international conference on computer vision (ICCV)*, pages 9627–9636, 2019.
- [Wang *et al.*, 2017] Zhe Wang, Yanxin Yin, Jianping Shi, Wei Fang, Hongsheng Li, and Xiaogang Wang. Zoom-in-net: Deep mining lesions for diabetic retinopathy detection. In *MICCAI*, pages 267–275. Springer, 2017.
- [Wang *et al.*, 2022] Kuo Wang, Yuxiang Nie, Chaowei Fang, Chengzhi Han, Xuewen Wu, Xiaohui Wang, Liang Lin, Fan Zhou, and Guanbin Li. Double-check soft teacher for semi-supervised object detection. In *IJCAI*, 2022.
- [Wen *et al.*, 2022] Hao Wen, Wenjian Yu, Yuanqing Wu, Zhao Jun, Xiaolong Liu, Zhexiang Kuang, and Rong Fan. Acne detection and severity evaluation with interpretable convolutional neural network models. *Technology and Health Care*, pages 1–11, 2022.
- [Wu *et al.*, 2019a] Xiaoping Wu, Ni Wen, Jie Liang, Yukun Lai, Dongyu She, Ming-Ming Cheng, and Jufeng Yang. Joint acne image grading and counting via label distribution learning. In *Proceedings of the IEEE international conference on computer vision (ICCV)*, pages 10642–10651, 2019.
- [Wu *et al.*, 2019b] Yuxin Wu, Alexander Kirillov, Francisco Massa, Wan-Yen Lo, and Ross Girshick. Detectron2. <https://github.com/facebookresearch/detectron2>, 2019.
- [Wu *et al.*, 2020] Yue Wu, Yinpeng Chen, Lu Yuan, Zicheng Liu, Lijuan Wang, Hongzhi Li, and Yun Fu. Rethinking classification and localization for object detection. In *Proceedings of the IEEE conference on computer vision and pattern recognition (CVPR)*, pages 10186–10195, 2020.
- [Xie *et al.*, 2017] Saining Xie, Ross Girshick, Piotr Dollár, Zhuowen Tu, and Kaiming He. Aggregated residual transformations for deep neural networks. In *Proceedings of the IEEE conference on computer vision and pattern recognition (CVPR)*, pages 1492–1500, 2017.
- [Xiong *et al.*, 2022] Feng Xiong, Jiayi Tian, Zhihui Hao, Yulin He, and Xiaofeng Ren. Scmt: Self-correction mean teacher for semi-supervised object detection. In *IJCAI*, 2022.
- [Yan *et al.*, 2020] Ke Yan, Jinzheng Cai, Youjing Zheng, Adam P Harrison, Dakai Jin, Youbao Tang, Yuxing Tang, Lingyun Huang, Jing Xiao, and Le Lu. Learning from multiple datasets with heterogeneous and partial labels for universal lesion detection in ct. *IEEE Transactions on Medical Imaging (TMI)*, 40(10):2759–2770, 2020.
- [Zaenglein, 2018] Andrea L Zaenglein. Acne vulgaris. *New England Journal of Medicine*, 379(14):1343–1352, 2018.